Suspended Sediment in the Surf Zone

By Rolf Deigaard,[1] Jørgen Fredsøe,[2] and Ida Brøker Hedegaard[3]

Abstract: The vertical distribution of suspended sediment under broken waves is considered. Close to the seabed, the turbulence is dominated by the wave-boundary layer, which determines the amount of suspended sediment very close to the bottom. Away from the bottom, the main contribution to the turbulence intensity originates from the surface generated turbulence due to wave breaking. This is described by application of the transport equation for turbulent kinetic energy. The production of kinetic energy is estimated from the energy loss in a hydraulic jump. The vertical distribution of suspended sediment is obtained from the diffusion equation. The theoretical findings are compared with laboratory experiments and field measurements.

Introduction

While much research has been carried out on the hydrodynamics in the surf zone, research on sediment transport mechanism is still at a preliminary stage. In *non-breaking waves*, suspended sediment is confined to the thin near-bed wave-boundary layer, as no turbulence is generated in the potential flow outside the wave-boundary layer. The vertical distribution of suspended sediment for this case has been solved by Bakker (2), Grant and Glenn (9), and Fredsøe, et al. (7). In all the aforementioned works, the vertical distribution of suspended sediment is found from the diffusion equation

$$\frac{\partial c}{\partial t} = w\frac{\partial c}{\partial y} + \frac{\partial}{\partial y}\left(\epsilon_s \frac{\partial c}{\partial y}\right) \quad (1)$$

where c = concentration by volume; t = time; w = fall velocity of suspended sediment; y = vertical coordinate; and ϵ_s = turbulent exchange factor for suspended sediment, which in Ref. 2 as well as in Ref. 7 is taken equal to the eddy viscosity ϵ of the flow. The difference between Ref. 2 and Ref. 7 is partly in the flow description, partly in the boundary condition for the bed concentration of suspended sediment. Bakker (2) develops the flow model by use of the mixing-length hypothesis, which in a later work, Bakker and van Doorn (3), is extended to cover the two-dimensional wave-current situation. Fredsøe, et al. (7) apply the model by Fredsøe (6), in which the boundary layer is regarded as a growing boundary layer in time during each half wave period. The model by Fredsøe is able to cover the general three-dimensional flow situation, where the current forms an arbitrary angle to the direction of the wave

[1]Hydr. Engr., Danish Hydraulic Inst., Agern Alle 5, DK-2970 Hørsholm, Denmark.

[2]Assoc. Prof., Inst. of Hydrodynamics and Hydraulic Engineering, (ISVA), Technical Univ. of Denmark, Bldg. 115, DK-2800 Lyngby, Denmark.

[3]ISVA. (Present address; Danish Hydraulic Inst.)

Note.—Discussion open until June 1, 1986. To extend the closing date one month, a written request must be filed with the ASCE Manager of Journals. The manuscript for this paper was submitted for review and possible publication on February 28, 1985. This paper is part of the *Journal of Waterway, Port, Coastal and Ocean Engineering*, Vol. 112, No. 1, January, 1986. ©ASCE, ISSN 0733-950X/86/0001-0115/$01.00. Paper No. 20324.

fronts. This is in fact the case in the surf zone, where the longshore current is parallel to the coast, while the wave orthogonals are nearly perpendicular to the coast.

The model by Grant and Glenn (9) applies the hydrodynamic description by Grant and Madsen (8) to describe the variation in eddy viscosity. Here, the eddy viscosity is taken to be constant with time. The model (9) includes a discussion of the effect of vertical density gradients due to the presence of suspended sediment and further allows wave ripples to be present on the bed, which is an extension compared to Refs. 2 and 7.

The purpose of the present investigation is to extend the work by Fredsøe, et al. (7) to include a description of the distribution of sediment in broken waves.

In *broken waves*, turbulent kinetic energy is produced in the roller at the surface as well as at the bottom in the wave boundary layer. Hereby, the eddy viscosity becomes much larger outside the wave boundary layer, so that more sediment can be carried in suspension away from the bed.

The following restrictions are introduced in the analysis:

1. The bed is assumed to be plane. At small values of the effective dimensionless bed shear stress θ', the bed is covered by small ripples. θ' is defined by

$$\theta' = \frac{\tau_b'}{\rho g d(s-1)} \qquad (2)$$

in which τ_b' = effective maximum bed shear stress; ρ = fluid density; g = acceleration of gravity; d = mean grain diameter; and s = relative density of sediment. For θ' values larger than 0.8–1.0, at which the largest rate of littoral drift usually takes place, the ripples disappear, so that the bed becomes plane (Nielsen, Ref. 12).

2. The type of breaking is assumed to be the spilling breaker. The conditions near the front of a spilling breaker are very much similar to a hydraulic jump. An experimental investigation by Rouse, Siao and Nagaratnam (14) has shown that the production of turbulent kinetic energy in the hydraulic jump is concentrated near the separated zone, the surface roller. This finding is also used in the present description of the spilling breaker. In case of a plunging breaker, the wave top is converted into a jet which splashes through the water surface so that turbulent energy may be produced over the entire depth. However, each plunging breaker breaks in a quite narrow zone after which the plunging breaker as well as the spilling breaker continue to move as a broken wave, in which the production of turbulent energy mainly takes place near the surface roller.

Suspended Sediment in Non-Breaking Waves

This problem is investigated in detail by Fredsøe, et al. (7). In case of *pure waves* only, the sediment is carried in suspension in the thin turbulent wave boundary layer just above the bed.

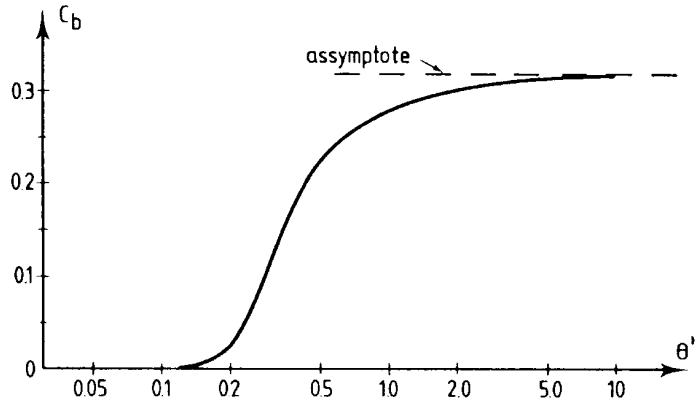

FIG. 1.—Reference Concentration at Bed c_b versus θ' (In Unsteady Motion, Instantaneous Value of θ' Is Applied)

The bed concentration of suspended sediment is based on the model by Engelund and Fredsøe (5), who apply the dynamic principles by Bagnold (1) to predict the concentration very close to the bottom. This model gives the bed concentration c_b—defined as the concentration at a distance of two grain diameters above the bed—as a function of θ' (Fig. 1).

It turned out from the analysis (7) that suspended sediment in pure wave motion is restricted to a layer of thickness only a few hundred times the grain diameter in agreement with laboratory test as well as field measurements [see Ref. 7, (Fig. 5)].

In combined *wave-current* motion, considerable amounts of turbulent energy are produced in a much larger region away from the bed as compared with the pure wave motion. Hereby, the eddy viscosity becomes significant over the total flow depth, so that suspended sediment may now exist in a much thicker layer above the bed, dependent on the fall velocity of sediment and the strength of the current. However, because the wave boundary layer is very thin, the bed shear stress is normally dominated by the waves unless the strength of the current is very large compared with the maximum wave-induced flow velocity. Usually, the near-bed wave motion is dominating in the sea. This means that close to the bed, the concentration of suspended sediment is determined by the waves, while the current may be important for the amount of suspended sediment farther away from the bed. Figs. 10 and 11, Ref. 7, show this very clearly.

Suspended Sediment under a Spilling Breaker

The turbulence generated in the water surface by broken waves has the same effect as the current, i.e., that more sediment is carried in suspension away from the bed, while the near-bed concentration is still determined by the wave boundary layer. The importance of this effect compared with that of the current depends on several parameters such as the height of the broken wave relative to the water depth and the strength of the current relative to the orbital wave velocity. Further, while the production of turbulent energy due to current is mainly concentrated

close to the bed, the production of turbulent energy as in spilling breakers is concentrated near the water surface, from which the turbulent energy is transported downwards in the fluid by diffusion.

In the following, the turbulence formed under a spilling breaker is investigated.

During the last years, much research has been going on about the surf zone dynamics. For instance, Madsen and Svendsen (11) and Svendsen and Madsen (17) have considered the gross behavior of the waves in the surf zone by application of depth integrated turbulence models, using similarity profiles for the vertical distribution of velocities and shear stress. For the present prupose a more detailed solution of the turbulent energy equation is needed in order to describe the vertical distribution of turbulence under broken waves.

Solution of k-Equation

In a broken wave, the turbulence is formed in the surface roller and spread by convection and diffusion. Because the location of the production is well-defined in time and space, the equation of motion can as a first approximation be avoided. Normally, the equation of motion is applied to calculate the production term in the transport of turbulent energy.

The transport equation for turbulent kinetic energy is given by

$$\frac{\partial k}{\partial t} = \frac{\partial}{\partial y}\left(\frac{\epsilon}{\sigma_k}\frac{\partial k}{\partial y}\right) + \frac{\mathrm{PROD}}{\rho} - c_d\frac{k^{3/2}}{l} \quad (3)$$

in which l is the length scale of turbulence; and σ_k and c_d are constants which in accordance with Launder and Spalding (10) are chosen as $\sigma_k = 1.0$ and $c_d = 0.08$. Finally, PROD in Eq. 3 stands for the production of turbulent energy.

In Eq. 3, the horizontal advection and diffusion terms are neglected. It is justified to neglect the horizontal diffusion in shallow water waves, because the horizontal length scale (the wave length L) is very large compared with the vertical length scale (the water depth D). Similar relations are valid for the advection where the velocity of the water particles outside the roller is much smaller than the migration velocity of the wave. Further on, the wave orbital motion will result in almost zero displacement of a water particle during one wave period (excluding the small volume of water in the surface roller).

The variation of the wave characteristics in the direction of wave migration will for ordinary beach slopes be so gradual that it can be totally neglected in the present analysis.

The different elements in the description of the turbulence in a spilling breaker are shown in Fig. 2.

For a one-equation turbulence model the length scale of turbulence l must be prescribed. In the upper part of the flow the presence of the bed has minor influence on the turbulence. Under conditions corresponding to free turbulence the length scale is almost constant and is of the order of magnitude $0.1D$ [Launder and Spalding (10)]. A constant

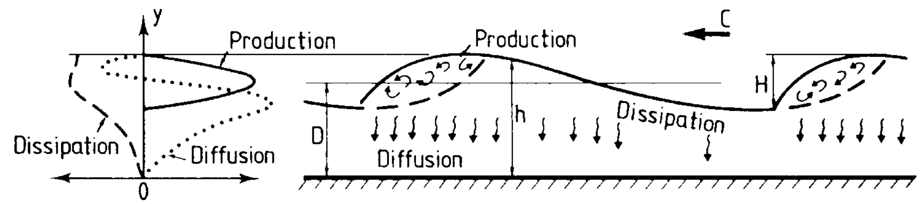

FIG. 2.—Definition Sketch Describing Elements Involved in Modeling of Turbulence (to the Left, Time-Averaged Values of Production, Vertical Diffusion, and Dissipation of Turbulent Energy Are Shown)

value of 0.07 D has been chosen on the basis of comparison of the present calculations with the turbulent measurements by Stive (16).

Close to the bed, the length scale of the turbulence will be reduced by the proximity of the bed. In this lower region a linear variation with the distance from the bed has been applied, similar to the near-bed variation of l in case of boundary layer flow. The length scale of turbulence, l, appearing in Eq. 3 is thus given by

$$l = \begin{cases} c_d^{1/4}\,\kappa y & \text{for} \quad y \le \dfrac{0.07\,D}{(c_d{}^{1/4})} \\ 0.07\,D & \text{for} \quad y > \dfrac{0.07\,D}{(c_d{}^{1/4})} \end{cases} \quad \ldots\ldots (4)$$

where κ is the von Kármán constant ($\sim$0.4); D = mean water depth; and y = distance from bed.

The turbulent eddy viscosity ϵ is given by

$$\epsilon = l\sqrt{k} \quad \ldots\ldots (5)$$

As previously mentioned, the location of the production of turbulent energy (PROD appearing in Eq. 3) is well-defined, see e.g., Ref. 11. In the present case, it is explicitly based on the wave characteristics, and is taken equal the energy loss in a bore or a hydraulic jump. Here the loss per unit bed area during one wave period is given by

$$E_{\text{loss}} = \Delta H \gamma D \quad \ldots\ldots (6)$$

where γ is the specific gravity; and ΔH = the head loss in a hydraulic jump with the same height H as the wave

$$\Delta H = \frac{H^3}{(4D^2 - H^2)} \quad \ldots\ldots (7)$$

The location of the energy production in the roller is obtained as follows: The depth integrated production $(\text{PROD})_{\text{mean}}$ is shown by Rouse, et al. (14) to be concentrated over a distance of two times the depth downstream of the toe of the jump (see Fig. 3). The dashed line in Fig. 3 shows the present approximation, which is taken as a parabola. The distribution of PROD over the vertical is also taken as a parabolic variation, vanishing at the water surface and one wave height beneath the surface as sketched in Fig. 2. This latter is also supported by the measurements by Rouse, et al. (14). Hereby, the variation in PROD with

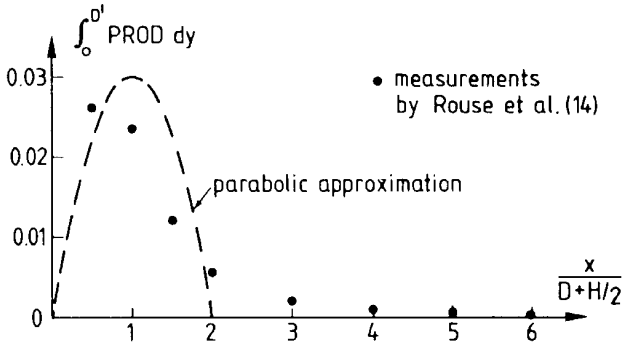

FIG. 3.—Measured and Approximated Depth-Integrated Production of Turbulent Energy in Hydraulic Jump

time and depth is given by

$$\text{PROD} = E_{\text{loss}} \frac{36}{(H\beta T)^2} z \left(1 - \frac{z}{H}\right) t \left(1 - \frac{t}{\beta T}\right) \quad \ldots\ldots\ldots\ldots\ldots\ldots\ldots\ldots \quad (8)$$

for t smaller than βT, where β is the part of the total time during which production of turbulent energy takes place

$$\beta = 2 \frac{\left(D + \frac{H}{2}\right)}{L} \quad \ldots\ldots\ldots\ldots\ldots\ldots\ldots\ldots\ldots\ldots\ldots\ldots\ldots\ldots\ldots\ldots\ldots\ldots \quad (9)$$

In Eq. 8, z is a vertical coordinate directed downwards with origin at the surface; and t is time starting with zero at each passage of a wave front.

Now, the transport equation can be solved by numerical integration with the two boundary conditions

$$k = 0 \quad \text{at} \quad y = 0 \quad \ldots\ldots\ldots\ldots\ldots\ldots\ldots\ldots\ldots\ldots\ldots\ldots\ldots\ldots\ldots\ldots\ldots\ldots \quad (10)$$

corresponding to k decreasing to zero at the bed (in contrast to bottom-generated turbulence where k approaches a finite value because the production at the bottom becomes infinite), and

$$\frac{\partial k}{\partial y} = 0 \quad \text{at} \quad y = D' \quad \ldots\ldots\ldots\ldots\ldots\ldots\ldots\ldots\ldots\ldots\ldots\ldots\ldots\ldots\ldots\ldots\ldots\ldots \quad (11)$$

corresponding to no energy flux through the water surface. D' is the local water depth.

Eq. 3 is solved numerically by application of the finite difference method. The equation is solved for a sufficient number of wave periods to reach a periodic solution irrespective of the initial condition. Fig. 4 shows a dimensionless plot of time-averaged turbulent kinetic energy for different combinations of dimensionless parameters.

Examples of the results from the model are given in Fig. 5 showing the calculated values of the root mean square of the horizontal velocity

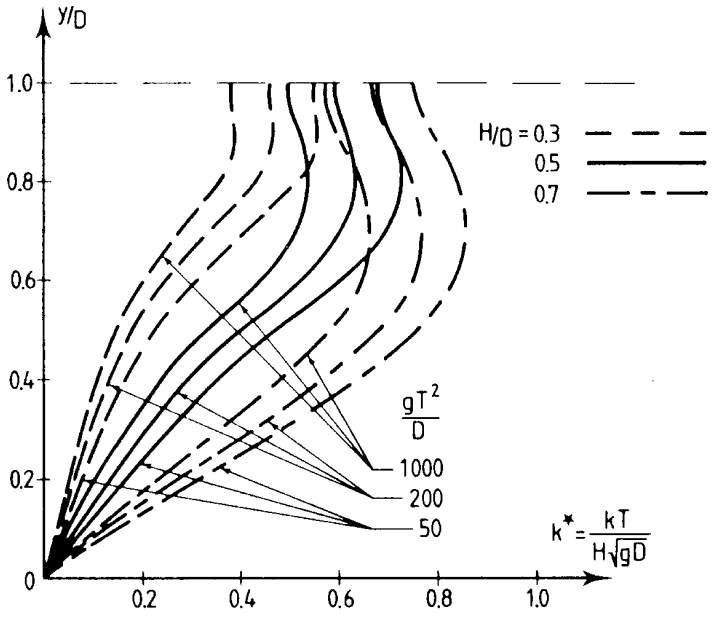

FIG. 4.—Variation over Depth of Dimensionless Time-Averaged Turbulent Energy k^* at Different Values of gT^2/D

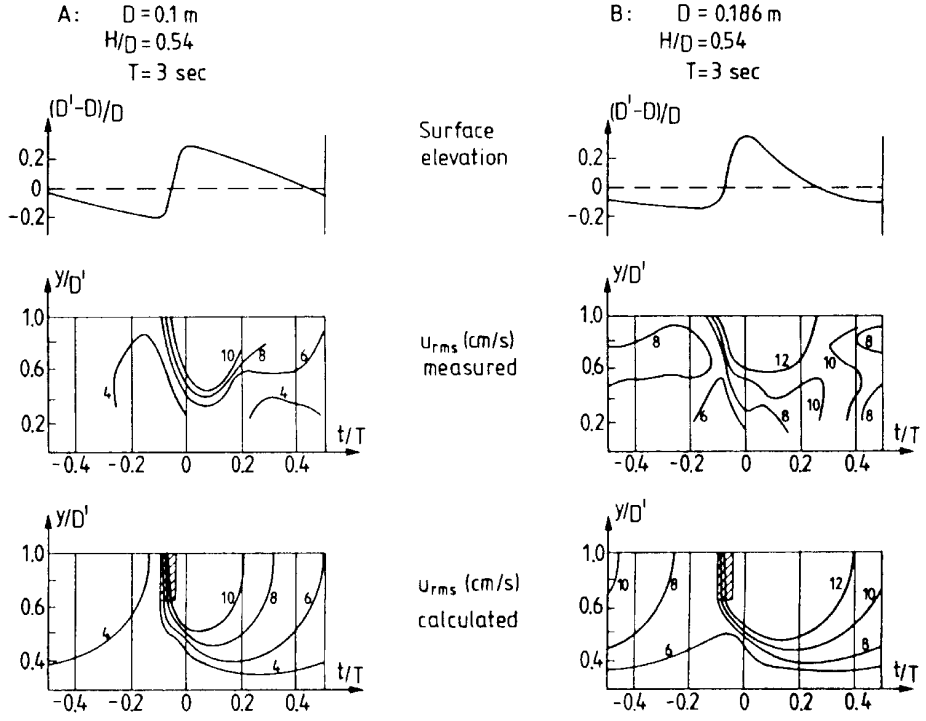

FIG. 5.—Measured (16) and Calculated Distribution of Turbulence: (*a*) D = 0.1 m, H/D = 0.54, T = 3 sec; (*b*) D = 0.186 m, H/D = 0.54, T = sec; (Shaded Areas in Lower Figures Show Zones of Production of Turbulence)

fluctuations u_{rms} together with measurements by Stive (16). In the calculations u_{rms} has been evaluated as $\sqrt{2k/3}$ corresponding to isotropic turbulence.

Vertical Distribution of Sediment

The concentration profile of suspended sediment under a spilling breaker can now be obtained by the same methodology as that applied by Fredsøe, et al. (7) by numerical solution of Eq. 1. At the instantaneous surface, the vertical flux of sediment is required to be zero. Eq. 1 is like Eq. 3 solved for sufficiently long time to produce periodic solution. The total eddy viscosity ϵ is in the present estimated by

$$\epsilon^2 = \epsilon_b^2 + \epsilon_t^2 \quad \ldots\ldots (12)$$

where ϵ_b = eddy viscosity formed by production of energy in the combined wave-current motion; and ϵ_t = eddy viscosity formed by the production of turbulent kinetic energy in the water surface. As seen from Eq. 5, Eq. 12 corresponds to taking the total turbulent kinetic energy as the sum of the bottom and surface generated turbulent energy, because the length scale of both kind of turbulence in the wall boundary layer may be expected to be described by Eq. 4, due to the effect of the wall proximity.

Fig. 6 shows dimensionless plots of the relative vertical distribution of time-averaged suspended sediment concentration due to the wave breaking only for three different wave heights at different wave periods. The concentration is normalized with c_0, the concentration 0.025 times the water depth above the bed. The curves plotted in Fig. 6 are not valid inside the wave boundary layer.

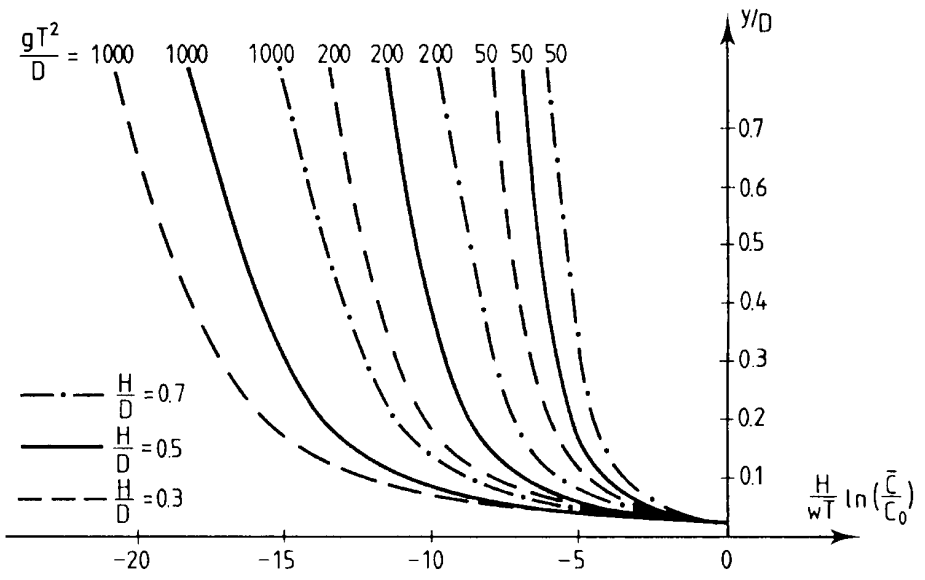

FIG. 6.—Theoretical Vertical Distribution of Suspended Sediment

Comparison with Measurements

In this section, a comparison with experiments, partly from the laboratory, partly from the field, is carried out.

The bed shear stress applied for calculation of θ' in the following is based on the model by Fredsøe (6). The near bed wave orbital motion is part of the input for this model in order to calculate the bed shear stresses and the characteristics of the wave and current boundary layer. Today no complete wave theory is available for the surf zone. Stive (16) has after a comprehensive experimental study concluded that the linear (Airy) wave theory gives a reasonable prediction of the velocity amplitude of the orbital motion. The calculations are therefore at the present based on the Airy wave theory. The comparative success of the simple linear theory is attributed to the more "full" profile of spilling breakers

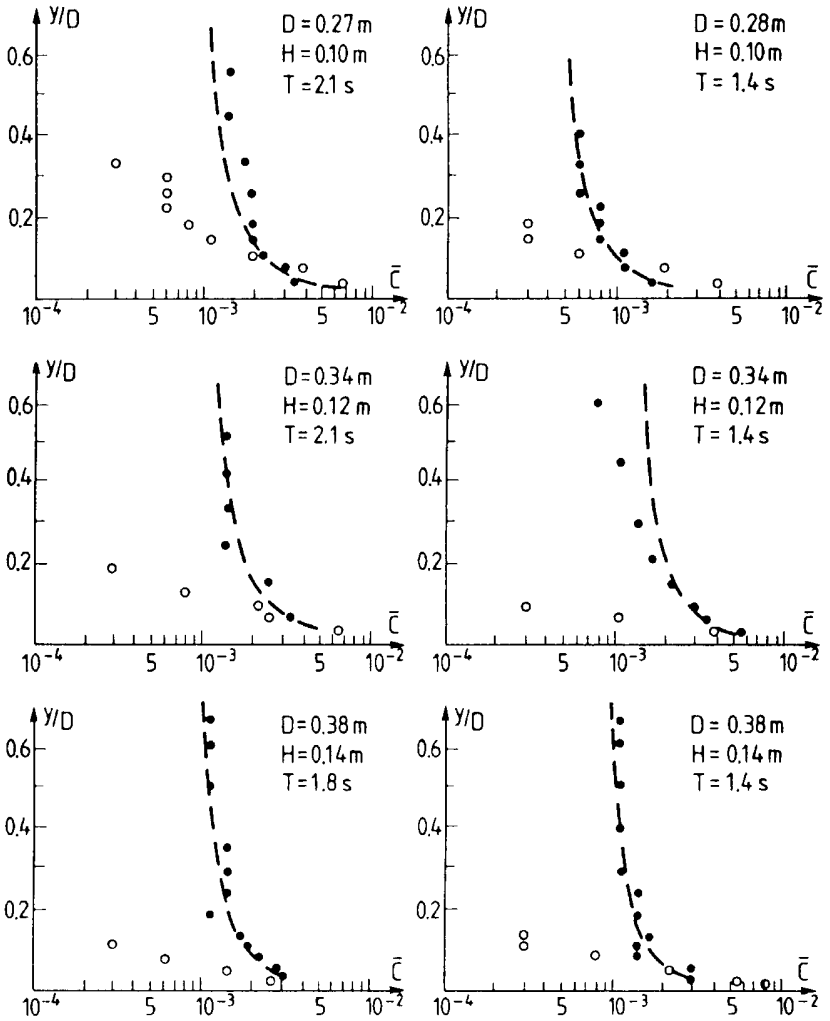

FIG. 7.—Comparison between Theory (Dashed) and Measured Time-Averaged Concentrations over Ripple-Covered Bed (●: Broken Waves; ○: Non-Breaking Waves)

and broken waves compared to waves which are near breaking.

Laboratory Test.—It is very difficult to obtain data from the laboratory because of the requirement of a plane bed or $\theta' > 0.8$–1.0. In case of non-breaking waves, these can be simulated by the flow in an oscillating flume as done, e.g., in Ref. 15. This can, of course, not be done in the case of breaking waves, so real waves must be applied. Due to restricted water depth in the flumes we have instead carried out experiments over a ripple-covered bed, where the concentration of suspended sediment is measured under spilling breakers as well as under non-breaking waves. In the two kinds of experiment, water depth, wave height, and wave period have been kept nearly identical in order to conpare the effect of breaking. The breaking of the waves has been provoked by a steep bed

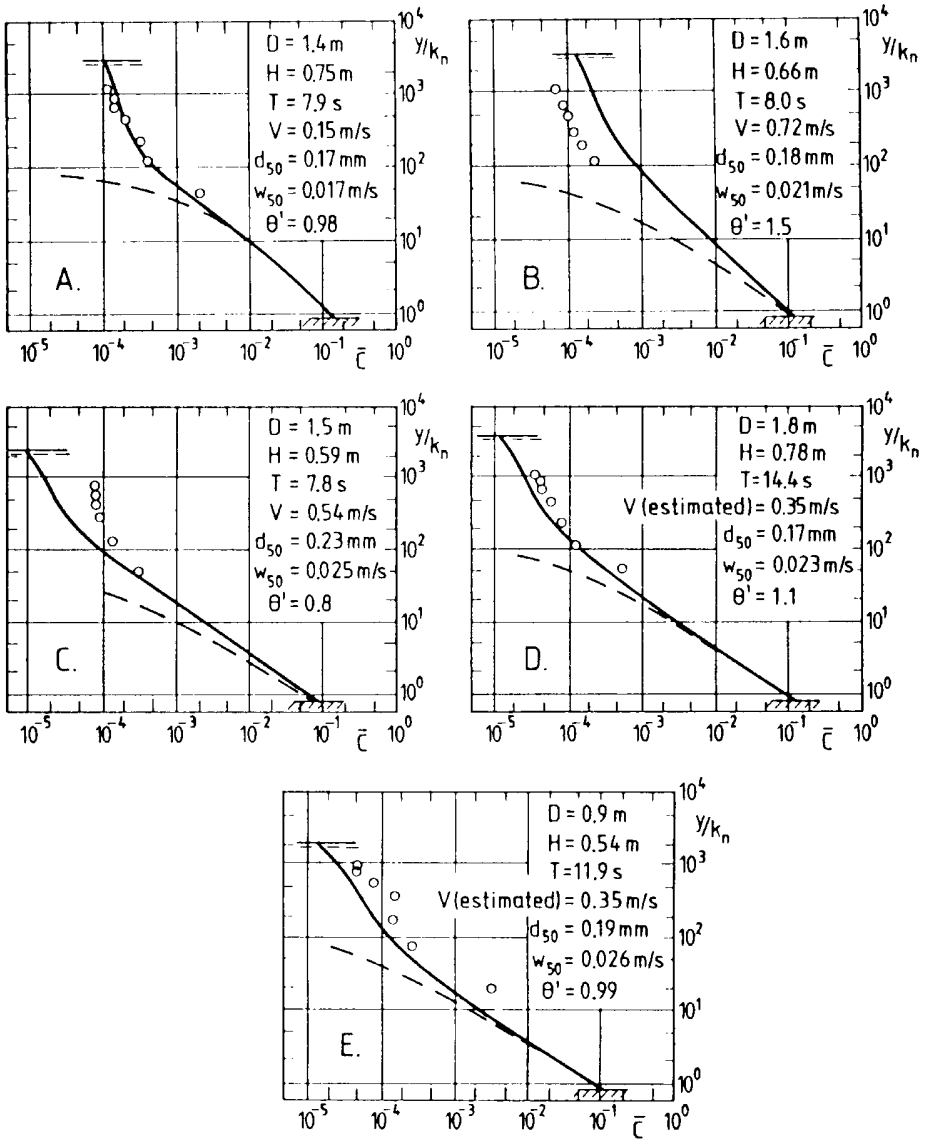

FIG. 8.—Comparison with Field Measurements (13) for Spilling Breaker Case

slope (1:12). The concentration measurements were taken about 3 m "downwave" of the slope where also the wave characteristics are measured. The concentration measurements were made by use of an optical instrument "Opcon," Bosman (4).

Fig. 7 shows the measured mean concentration in six different runs. Each point covers 20 wave periods. The dotted line is the theoretical prediction of the concentration of suspended sediment away from the bed under a spilling breaker. As no satisfactory theory exists for the near-bed sediment concentration profile over ripple beds, the boundary conditions for the model are not known, and the calculated profiles have been made to fit the lower points of the concentration measurements. The mean diameter of the sand in the runs is 0.12 mm.

The relative distribution of suspended sediment is reasonably well described by the theory.

It is interesting to note that the near-bed mean concentration is nearly the same under the spilling breaker as under non-breaking waves, as already noticed by Nielsen (12). This confirms that the near-bed concentration is determined by the bottom boundary layer.

Field Measurements.—In the field, the bed in the surf zone usually becomes plane (no ripples) when heavy wave action occurs. Nielsen, et al. (13) have measured the concentration of suspended sediment on several locations in Australia by use of a suction sampling system. The suction is carried out at different levels above the bed, and simultaneous

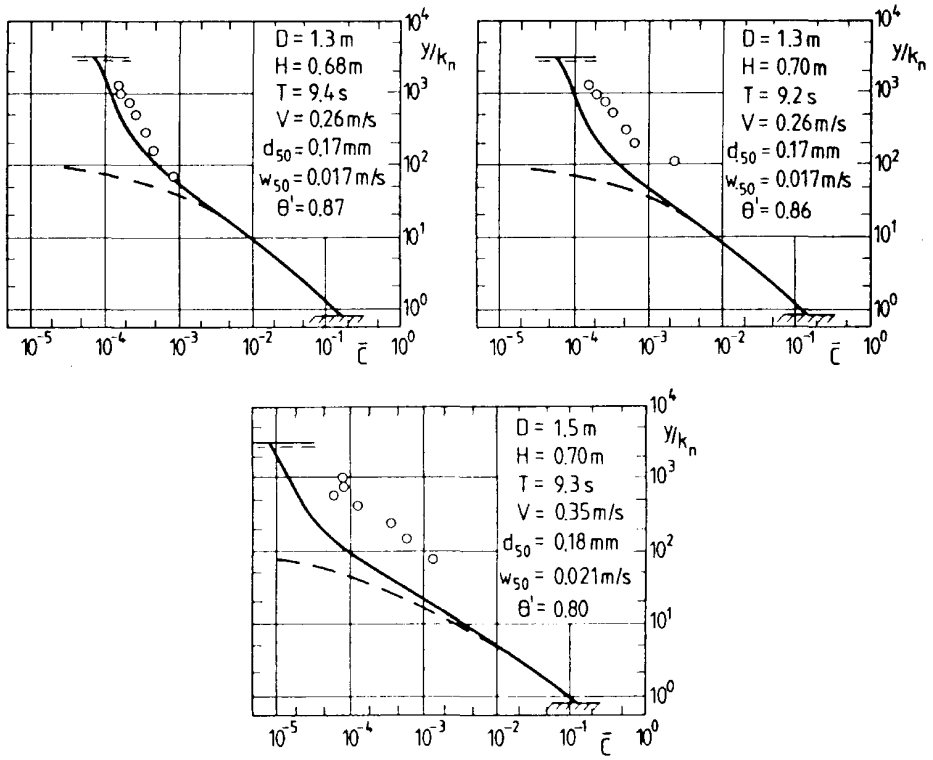

FIG. 9.—Comparison between Theory and Field Measurements (11) for Plunging Breaker Case (Symbols as in Fig. 8)

measurements of wave height, wave period, current strength, and current direction have been performed. Figs. 8 and 9 show a comparison between the measured and the predicted mean averages concentrations of suspended sediment. Only the data, where $\theta' > 0.8$ are included in order to ensure that the bed becomes nearly plane. Comparison with spilling as well as plunging breakers have been carried out.

Fig. 8(*a–c*) shows three measurements for the spilling breaker case in which the current as well as the waves are measured. Keeping in mind that these are field measurements, the agreement is reasonable (within a factor three). The full-drawn line shows the complete theory, while the dashed line shows the theoretical finding for the wave boundary only (without turbulence from current and wave breaking).

Finally, Fig. 8(*d–e*) shows two field measurements from the spilling breaker case, where the effective Shields parameter is so large that ripples are expected not to occur, but where only the wave climate and not the strength of the current is measured. Here, we have taken the current velocity equal to the mean of all the measured current velocities.

Fig. 9 shows three measurements, where the waves are characterized as plunging breakers. Here, the theory which is not intended to describe the conditions at the plunge point, slightly underpredicts the concentrations as expected.

Conclusion

A mathematical model has been developed to describe the vertical distribution of suspended sediment under spilling breakers. The near-bed concentrations are determined by the turbulence and shear stresses formed in the wave boundary layers. Farther away from the bed, the surface generated turbulence, which is transported downwards by diffusion, is responsible for large amounts of sediment being kept in suspension. The calculated vertical distribution is supported by laboratory and field measurements.

Acknowledgments

One of the writers (R.D.) is supported by the Danish Technical Research Council (STVF). The "OPCON"-meter was made freely available by J. Bosman, Delft Hydraulic Laboratory.

Appendix I.—References

1. Bagnold, R. A., "Experiments on a Gravity-Free Dispersion of Large Solid Spheres in a Newtonian Fluid under Shear," *Proceedings, Royal Society*, London, England, Ser. A, 225, 1954, p. 49.
2. Bakker, W. T., "Sand Concentration in an Oscillatory Flow," Coastal Engineering Conference, 1974, pp. 1129–1148.
3. Bakker, W. T., and Doorn, Th., "Near-Bottom Velocities in Waves with a Current," Coastal Engineering Conference, 1978, pp. 1394–1413.
4. Bosman, J., "Calibration of Optical Systems for Sediment Concentration Measurements," Delft Hydraulics Lab., R 716, Part V, 1983.
5. Engelund, F., and Fredsøe, J., "A Sediment Transport Model for Straight Alluvial Channels," *Nordic Hydrology*, Vol. 7, 1976, pp. 293–306.

6. Fredsøe, J., "Turbulent Boundary Layer in Wave and Current Motion," *Journal of Hydraulic Engineering*, ASCE, Vol. 110, No. 8, 1984, pp. 1103–1120.
7. Fredsøe, J., Andersen, O. H., and Silberg, S., "Distribution of Suspended Sediment in Large Waves," *Journal of Waterway, Port, Coastal and Ocean Engineering*, ASCE, Nov., 1985.
8. Grant, W. D., and Madsen, O. S., "Combined Wave and Current Interaction with a Rough Bottom," *Journal of Geophysical Research*, Vol. 84, 1979, pp. 1797–1808.
9. Grant, W. G., and Glenn, S. M., "Continental Shelf Bottom Boundary Layer Model, Vol. I: Theoretical Model Development," Woods Hole Oceanographic Institution, Ocean Engineering Dept., 1983.
10. Launder, B. E., and Spalding, D. B., "Mathematical Models of Turbulence," Academic Press, London and New York, 1972.
11. Madsen, P. A., and Svendsen, I. A., "Turbulent Bores and Hydraulic Jumps," *Journal of Fluid Mechanics*, Vol. 129, 1983, pp. 1–25.
12. Nielsen, P., "Some Basic Concepts of Wave Sediment Transport," Institute of Hydrodynamics and Hydraulic Engineering, Technical Univ. of Denmark, Series Paper 20, 1979.
13. Nielsen, P., Green, M. O., and Coffey, F. C., "Suspended Sediment under Waves," Department of Geography, The Univ. of Sidney, Coastal Studies Unit, *Technical Report No. 8216*, 1982.
14. Rouse, H., Siao, T. T., and Nagaratnam, S., "Turbulence Characteristics of the Hydraulic Jump," *Proceedings*, ASCE, Vol. 84, No. HY1, 1958, pp. 1–30.
15. Staub, C., Svendsen, I. A., and Jonsson, I. G., "Measurements of the Instantaneous Sediment Suspension in Oscillatory Flow," *Progress Report 58*, Institute of Hydrodynamics and Hydraulic Engineering, Technical Univ. of Denmark, 1983, pp. 41–49.
16. Stive, M. J. F., "Velocity and Pressure Field of Spilling Breakers," *Proceedings 17th Coastal Engineering Conference*, 1980, pp. 547–566.
17. Svendsen, I. A., and Madsen, P., "A Turbulent Bore on a Beach," *Journal of Fluid Mechanics*, 148, 1984, pp. 73–96.

APPENDIX II.—NOTATION

The following symbols are used in this paper:

c = concentration of suspended sediment,
c_b = bed concentration of suspended sediment,
c_0 = concentration a distance 0.025 D above the bed,
c_d = constant appearing in Eq. 3 (= 0.08),
D = mean water depth,
D' = local water depth,
d = mean grain diameter,
E_{loss} = energy loss in a hydraulic jump,
g = acceleration of gravity,
H = wave height,
k = turbulent kinetic energy,
k^* = dimensionless version of k [= $kT/(H\sqrt{gD})$],
k_n = bed roughness (= $2.5d$),
L = wavelength,
l = length scale of turbulence,
s = relative density of sediment,
T = wave period,
t = time,
u_{rms} = root mean square of turbulent velocity fluctuations,

V = mean current velocity,
w = mean fall velocity of suspended sediment,
y = distance from bed,
z = distance from surface,
β = relative time, defined in Eq. 9;
γ = specific fluid gravity,
ϵ = eddy viscosity,
ϵ_b = contribution to eddy viscosity from wave boundary layer and current,
ϵ_s = turbulent exchange factor for suspended sediment,
ϵ_t = contribution to eddy viscosity from production of turbulent kinetic energy in the roller,
η = local surface elevation,
θ' = dimensionless effective bed shear stress,
κ = von Kármán's constant (~0.4),
ρ = fluid density,
σ_k = constant appearing in Eq. 3 (~1.0), (Prandtl number); and
τ_b' = effective bed shear stress.